

# The frustrated spin-1/2 $J_1$ - $J_2$ Heisenberg ferromagnet on the square lattice: Exact diagonalization and Coupled-Cluster study

J. Richter<sup>1</sup>, R. Darradi<sup>2</sup>, J. Schulenburg<sup>3</sup>, D.J.J. Farnell<sup>4</sup>, and H. Rosner<sup>5</sup>

<sup>1</sup>Institut für Theoretische Physik, Universität Magdeburg, D-39016 Magdeburg, Germany

<sup>2</sup>Institut für Theoretische Physik, Technische Universität Braunschweig, D-38106 Braunschweig, Germany

<sup>3</sup>Universitätsrechenzentrum, Universität Magdeburg, D-39016 Magdeburg, Germany

<sup>4</sup>Academic Department of Radiation Oncology, University of Manchester, United Kingdom

<sup>5</sup>Max-Planck Institut für Chemische Physik fester Stoffe, D-01187 Dresden, Germany

November 26, 2024

## Abstract

We investigate the ground-state magnetic order of the spin-1/2  $J_1$ - $J_2$  Heisenberg model on the square lattice with ferromagnetic nearest-neighbor exchange  $J_1 < 0$  and frustrating antiferromagnetic next-nearest neighbor exchange  $J_2 > 0$ . We use the coupled-cluster method to high orders of approximation and Lanczos exact diagonalization of finite lattices of up to  $N = 40$  sites in order to calculate the ground-state energy, the spin-spin correlation functions, and the magnetic order parameter. We find that the transition point at which the ferromagnetic ground state disappears is given by  $J_2^{c1} = 0.393|J_1|$  (exact diagonalization) and  $J_2^{c1} = 0.394|J_1|$  (coupled-cluster method). We compare our results for ferromagnetic  $J_1$  with established results for the spin-1/2  $J_1$ - $J_2$  Heisenberg model with antiferromagnetic  $J_1$ . We find that both models (i.e., ferro- and antiferromagnetic  $J_1$ ) behave similarly for large  $J_2$ , although significant differences between them are observed for  $J_2/|J_1| \lesssim 0.6$ . Although the semiclassical collinear magnetic long-range order breaks down at  $J_2^{c2} \approx 0.6J_1$  for antiferromagnetic  $J_1$ , we do not find a similar breakdown of this kind of long-range order until  $J_2 \sim 0.4|J_1|$  for the model with ferromagnetic  $J_1$ . Unlike the case for antiferromagnetic  $J_1$ , if an intermediate disordered phase does occur between the phases exhibiting semiclassical collinear stripe order and ferromagnetic order for ferromagnetic  $J_1$  then it is likely to be over a very small range below  $J_2 \sim 0.4|J_1|$ .

PACS codes:

75.10.Jm Quantized spin models

75.45.+j Macroscopic quantum phenomena in magnetic systems

75.10.Kt Quantum spin liquids, valence bond phases and related phenomena

## 1 Introduction

The spin-1/2 Heisenberg antiferromagnet with nearest-neighbor (NN)  $J_1$  and frustrating next-nearest-neighbor (NNN)  $J_2$  coupling ( $J_1$ - $J_2$  model) on the square lattice has attracted much at-

tention during the last twenty years (see, e.g., Refs. [1–20] and references therein). This model may serve as a canonical model to study the interplay of frustration effects and quantum fluctuations as well as quantum phase transitions driven by frustration.

The corresponding Hamiltonian reads

$$H = J_1 \sum_{\langle i,j \rangle} \mathbf{s}_i \cdot \mathbf{s}_j + J_2 \sum_{\langle\langle i,j \rangle\rangle} \mathbf{s}_i \cdot \mathbf{s}_j, \quad (1)$$

where the sums over  $\langle i,j \rangle$  and  $\langle\langle i,j \rangle\rangle$  run over all NN and NNN pairs, respectively, counting each bond once.

Recently, several quasi-two-dimensional magnetic materials with a ferromagnetic (FM) NN coupling  $J_1 < 0$  and an antiferromagnetic (AFM) NNN coupling  $J_2 > 0$  have been studied experimentally, e.g.,  $\text{Pb}_2\text{VO}(\text{PO}_4)_2$  [21–24],  $(\text{CuCl})\text{LaNb}_2\text{O}_7$  [25],  $\text{SrZnVO}(\text{PO}_4)_2$  [24, 26, 27], and  $\text{BaCdVO}(\text{PO}_4)_2$  [23, 26, 28]. Due to a quite large AFM coupling  $J_2$  these materials are driven out of the FM phase. These experimental studies have stimulated a series of theoretical investigations of the ground state (GS) and thermodynamic properties of the FM  $J_1$ - $J_2$  model, i.e. the model with FM NN exchange  $J_1$  and frustrating AFM NNN exchange  $J_2$  [29–37]. It was found that the FM GS for the spin-1/2 model breaks down at  $J_2 = J_2^{c1} \approx 0.4|J_1|$  [29–31, 34, 37, 38]. Note that for the classical model ( $s \rightarrow \infty$ ) the corresponding transition point is at  $J_2 = 0.5|J_1|$ . Moreover, for sufficiently large  $J_2 > J_2^{c2}$  a magnetically long-range ordered collinear stripe GS appears. According to Refs. [30, 31, 35, 36] this second critical frustration strength is  $J_2^{c2} \approx 0.6|J_1|$ , and both magnetically ordered phases are separated by a magnetically disordered phase with enhanced nematic correlations. Note that this collinear stripe GS phase, as well as the values of  $J_2^{c1}$  and  $J_2^{c2}$  reported in the literature, are similar to the observation for the corresponding AFM model, i.e. the model with AFM  $J_1$  [1, 4, 6, 7, 9, 11–13, 15–20].

As we know from the investigation of the AFM  $J_1$ - $J_2$  model the study of the GS phases in the strong frustration regime, i.e.  $J_2 \sim 0.5J_1$ , is one of the hardest problems in the field of frustrated quantum magnetism. In the meantime, scores of papers have dealt with this problem. On the other hand, for the FM  $J_1$ - $J_2$  model so far only a few studies exist. Hence, further investigations using alternative approaches are highly desirable to confirm or to query the existing results.

Due to frustration, highly efficient quantum Monte-Carlo codes, such as the stochastic series expansion suffer from the minus sign problem. Therefore, many other approximate methods, e.g. the Green’s function method [10, 13, 37], the series expansion [11, 12, 17], the Schwinger boson approach [7], variational techniques [9], the functional renormalization group technique [20] as well as the projected entangled pair states method [18] were used to study the GS phases of the model with AFM  $J_1$ .

In the present paper we calculate the GS energy, spin-spin correlation functions, and the magnetic order parameter of the collinear stripe order using two completely different methods, namely a large-scale exact diagonalization (ED) of finite lattices up to  $N = 40$  sites (see Sec. 2) and the coupled-cluster method (CCM) (see Sec. 3). Both methods have been successfully applied to the AFM  $J_1$ - $J_2$  model, see e.g. Refs. [2–6, 19] for the ED method and Refs. [8, 13–16] for the CCM.

Henceforth we set  $|J_1| = 1$  if not stated otherwise explicitly.

## 2 Results of Lanczos exact diagonalization for finite square lattices

The paper of Schulz and co-workers [4], presenting results for finite lattices up to  $N = 36$  sites for the first time has set a benchmark for ED studies of quantum Heisenberg magnets. Frequently, such

Table 1: Singlet GS energy per site  $E_0/N$  and square of order parameter  $M_N^2(0, \pi)$ , cf. Eq. (2), for the  $J_1$ - $J_2$  model with  $J_1 = -1$  on finite square lattices of  $N = 32, 36$  and  $40$  sites.

|       | $N = 32$    | $N = 32$        | $N = 36$    | $N = 36$        | $N = 40$    | $N = 40$        |
|-------|-------------|-----------------|-------------|-----------------|-------------|-----------------|
| $J_2$ | $E_0/N$     | $M_N^2(0, \pi)$ | $E_0/N$     | $M_N^2(0, \pi)$ | $E_0/N$     | $M_N^2(0, \pi)$ |
| 0.40  | -0.31284253 | 0.11167341      | -0.31431081 | 0.08925821      | -0.31127637 | 0.10687524      |
| 0.45  | -0.34234578 | 0.12363200      | -0.34259033 | 0.11439947      | -0.34062128 | 0.11332095      |
| 0.50  | -0.37406800 | 0.12617129      | -0.37369533 | 0.11854042      | -0.37174835 | 0.11581048      |
| 0.55  | -0.40673497 | 0.12730259      | -0.40577614 | 0.12049011      | -0.40374930 | 0.11719238      |
| 0.60  | -0.43994975 | 0.12793318      | -0.43841728 | 0.12170653      | -0.43628038 | 0.11810286      |
| 0.65  | -0.47352394 | 0.12833506      | -0.47143169 | 0.12256200      | -0.46917022 | 0.11876286      |
| 0.70  | -0.50735237 | 0.12861459      | -0.50471467 | 0.12320526      | -0.50231993 | 0.11927048      |
| 0.80  | -0.57553353 | 0.12898259      | -0.57184472 | 0.12411474      | -0.56916790 | 0.12000667      |
| 0.90  | -0.64418634 | 0.12921694      | -0.63949153 | 0.12472863      | -0.63652042 | 0.12051714      |
| 1.00  | -0.71315309 | 0.12937976      | -0.70748822 | 0.12516916      | -0.70421577 | 0.12089143      |

numerical exact results are also used to test new approximate methods, see, e.g. Refs. [16, 39, 40]. Due to the progress in the computer hardware and the increased efficiency in programming, very recently the GS and low-lying excitations of the unfrustrated (i.e.,  $J_2 = 0$ ) [41] as well as the frustrated spin-1/2 HAFM [19] and of a spin-1/2 Heisenberg model with ring exchange [42] have been calculated by the Lanczos algorithm for a square lattice with  $N = 40$  sites. The largest two-dimensional quantum spin model for which the GS has been calculated so far is the spin-1/2 HAFM on the star lattice with  $N = 42$  sites [43]. Note, however, that for sectors of  $S_z > 0$  which are relevant for finite magnetic fields much larger system sizes can be treated by ED, see, e.g., Ref. [44].

In order to analyze GS magnetic ordering, the spin-spin correlation functions and an appropriate order parameter are important quantities. Following Schulz et al., [4] we use here the  $\mathbf{Q}$ -dependent susceptibility (square of order parameter) defined as

$$M_N^2(\mathbf{Q}) = \frac{1}{N(N+2)} \sum_{i,j} \langle \mathbf{s}_i \cdot \mathbf{s}_j \rangle e^{i\mathbf{Q}(\mathbf{R}_i - \mathbf{R}_j)}. \quad (2)$$

The relevant order parameter for the collinear stripe magnetic LRO present at large  $J_2$  is  $M_N^2(\mathbf{Q})$  at the magnetic wave vectors  $\mathbf{Q}_1 = (\pi, 0)$  or  $\mathbf{Q}_2 = (0, \pi)$ . In Table 1 we give the singlet GS energies per site as well as the order parameters  $M_N^2(0, \pi)$  for finite lattices of  $N = 32, 36$ , and  $40$  sites. In a second Table 2 we present the spin-spin correlation functions  $\langle \mathbf{s}_0 \cdot \mathbf{s}_{\mathbf{R}} \rangle$  for the largest lattice considered. There are in total 11 different correlation functions for  $N = 40$  that are given in Table 2 for the same data points as in Table 1. Periodic boundary conditions are imposed for all of the lattices employed here. A graphical representation of the finite lattices can be found in Refs. [4] and [19]. The exact data, which is provided here in some detail in the tables, might be used as benchmark data for approximate methods applied to this model.<sup>1</sup>

The corresponding data for the energies, the square of order parameters and for some selected correlation functions are also displayed in more detail in Figs. 1, 2, and 3. By way of comparison, we also present corresponding curves for the AFM model ( $J_1 = +1$ ) [19]. We recall that the GS

<sup>1</sup>The spin-spin correlation functions for  $N = 20, 32$ , and  $36$  can be provided upon request.

Table 2: Spin-spin correlation functions  $\langle \mathbf{s}_0 \cdot \mathbf{s}_{\mathbf{R}} \rangle$  for the  $J_1$ - $J_2$  with  $J_1 = -1$  model on the finite square lattice of  $N = 40$  sites.

|       | $\langle \mathbf{s}_0 \cdot \mathbf{s}_{\mathbf{R}} \rangle$ |
|-------|--|--|--|--|--|--|
| $J_2$ | $\mathbf{R} = (1, 0)$  | $\mathbf{R} = (2, 0)$  | $\mathbf{R} = (3, 0)$  | $\mathbf{R} = (3, 1)$  | $\mathbf{R} = (2, 1)$  | $\mathbf{R} = (1, 1)$  |
| 0.40  | 0.044832   | 0.183933   | 0.012219   | -0.194442  | -0.040218  | -0.277017  |
| 0.45  | 0.033144   | 0.196362   | 0.014787   | -0.199197  | -0.033852  | -0.304812  |
| 0.50  | 0.027648   | 0.201318   | 0.014973   | -0.200208  | -0.029595  | -0.316452  |
| 0.55  | 0.024204   | 0.204078   | 0.014523   | -0.200667  | -0.026460  | -0.323037  |
| 0.60  | 0.021753   | 0.205887   | 0.013884   | -0.201012  | -0.024012  | -0.327312  |
| 0.65  | 0.019875   | 0.207189   | 0.013203   | -0.201327  | -0.022023  | -0.330324  |
| 0.70  | 0.018363   | 0.208185   | 0.012537   | -0.201621  | -0.020367  | -0.332568  |
| 0.80  | 0.016044   | 0.209616   | 0.011328   | -0.202149  | -0.017745  | -0.335676  |
| 0.90  | 0.014313   | 0.210600   | 0.010293   | -0.202593  | -0.015750  | -0.337719  |
| 1.00  | 0.012954   | 0.211320   | 0.009417   | -0.202962  | -0.014172  | -0.339156  |

|       | $\langle \mathbf{s}_0 \cdot \mathbf{s}_{\mathbf{R}} \rangle$ |
|-------|--|--|--|--|--|
| $J_2$ | $\mathbf{R} = (1, 2)$  | $\mathbf{R} = (1, 3)$  | $\mathbf{R} = (2, 2)$  | $\mathbf{R} = (2, 3)$  | $\mathbf{R} = (4, -2)$                                       |
| 0.40  | -0.027909  | -0.177408  | 0.160527   | -0.007815  | 0.154329   |
| 0.45  | -0.023862  | -0.183867  | 0.176142   | -0.003522  | 0.166329   |
| 0.50  | -0.021057  | -0.186297  | 0.181923   | -0.002268  | 0.169644   |
| 0.55  | -0.018936  | -0.187719  | 0.185043   | -0.001671  | 0.171225   |
| 0.60  | -0.017247  | -0.188748  | 0.187071   | -0.001323  | 0.172227   |
| 0.65  | -0.015858  | -0.189567  | 0.188526   | -0.001098  | 0.172968   |
| 0.70  | -0.014691  | -0.190248  | 0.189642   | -0.000936  | 0.173562   |
| 0.80  | -0.012825  | -0.191325  | 0.191262   | -0.000723  | 0.174483   |
| 0.90  | -0.011394  | -0.192135  | 0.192387   | -0.000588  | 0.175173   |
| 1.00  | -0.010260  | -0.192765  | 0.193215   | -0.000498  | 0.175707   |

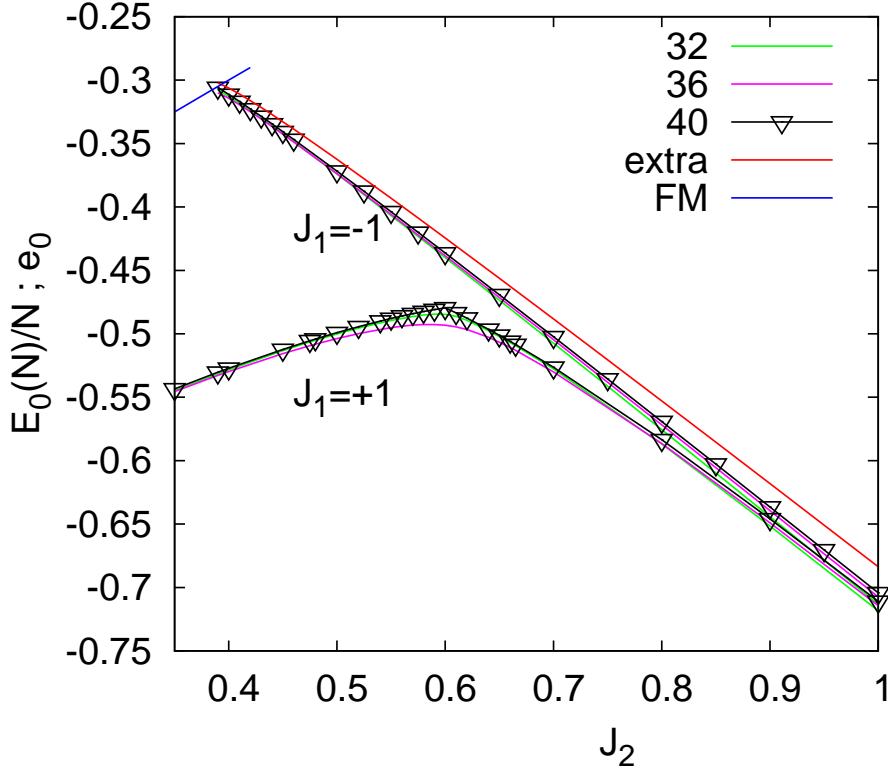


Figure 1: GS energy per site  $E_0(N)/N$  calculated by ED for finite lattices of  $N = 32, 36, 40$  sites as well as the extrapolated value  $e_0$  ( $N \rightarrow \infty$ ), cf. Eq. (3). For comparison we show also  $E_0(N)/N$  for the AFM model ( $J_1 = +1$ ) with  $N = 32, 36, 40$  [19]. The blue line shows the energy of the FM eigenstate.

is identical for the FM and the AFM model on the classical level for  $J_2 > 0.5$ . For the spin-1/2 model, due to quantum fluctuations, the two models behave differently. Only in the limit  $J_2 \rightarrow \infty$  the sign of  $J_1$  becomes irrelevant for the quantum GS. Our numerical data for the GS energy, the order parameter, and the spin-spin correlation functions demonstrate that for  $J_2 \gtrsim 0.8$  the different models behave qualitatively very similarly. Note, however, that due to the different sign in the NN exchange  $J_1$ , also the NN spin-spin correlation  $\langle \mathbf{s}_0 \cdot \mathbf{s}_{\mathbf{R}} \rangle$ ,  $\mathbf{R} = (1, 0)$ , has a different sign for the models. In the region  $0.8 \gtrsim J_2 \gtrsim 0.6$  the differences between both models become more and more pronounced. For  $J_2 \lesssim 0.6$  both models behave completely different. From many previous studies [1–19] we know that  $J_2 \approx 0.6$  is the point where for the AFM model the semiclassical collinear stripe LRO gives way for a magnetically disordered phase. It is obvious that at  $J_2 \approx 0.6$  the order parameter  $M_N^2(0, \pi)$  of the AFM model changes drastically (cf. Fig. 2, whereas  $M_N^2(0, \pi)$  remains almost constant up to about  $J_2 \approx 0.45$  for the FM model, i.e. there is no indication for a breakdown of semiclassical magnetic LRO around  $J_2 \approx 0.6$  for  $J_1 = -1$ . Only for  $J_2 \lesssim 0.45$  there is a noticeable decrease in the order parameter  $M_N^2(0, \pi)$  until the transition point  $J_2^{c1}$  between the singlet GS and the fully polarized FM GS. Note, however, that  $M_N^2(0, \pi)$  remains finite until  $J_2^{c1}$ . The different behavior of both models can also be seen in the GS energy and the spin-spin correlation functions, cf. Figs. 1 and 3. From Fig. 1 it is evident that the finite size-effects in the GS energy  $E_0$  of the FM model are small. In fact, the difference in  $E_0$  between  $N = 36$  and  $N = 40$  is less than 1% in the whole region shown in Fig. 1. Hence, a finite-size extrapolation should give accurate results for the GS energy (see below).

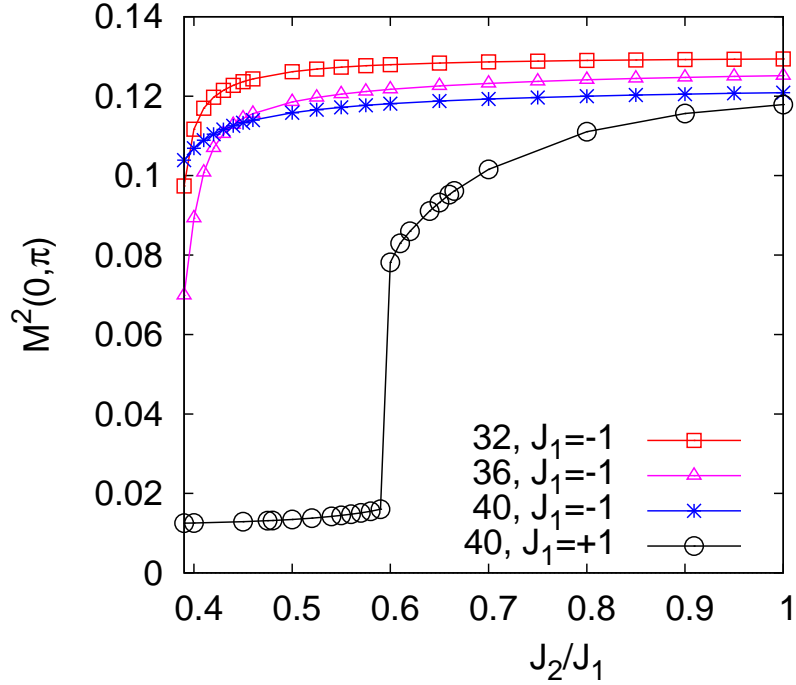


Figure 2: Square of order parameters  $M_N^2(0, \pi)$ , see Eq. (2), for  $N = 32, 36$ , and  $40$  ( $J_1 = -1$ ). For comparison we also present a corresponding curve for the AFM model ( $J_1 = +1$ ) for  $N = 40$ .

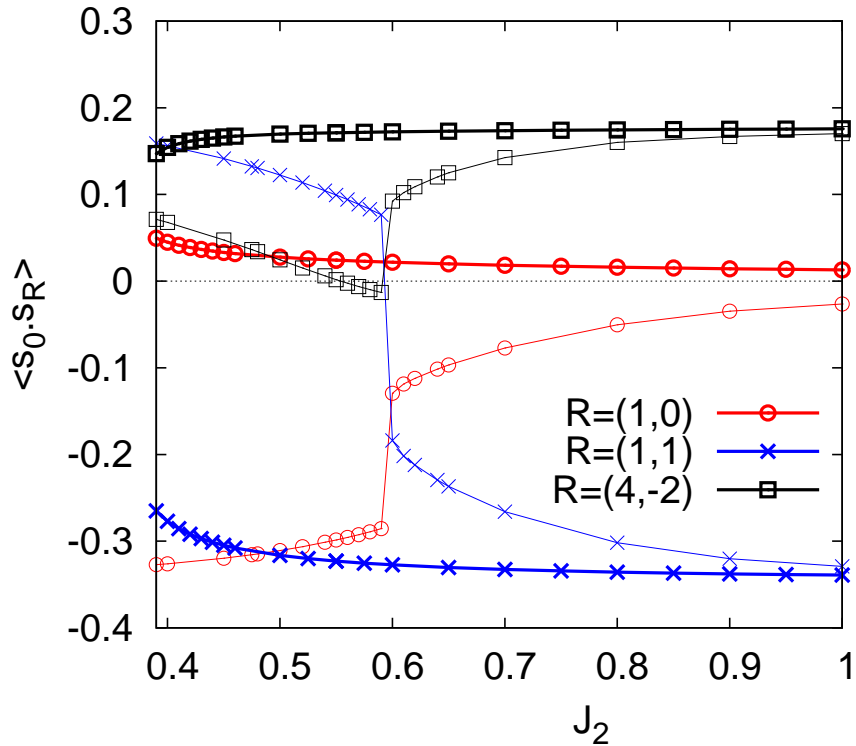


Figure 3: Selected spin-spin correlation functions  $\langle s_0 \cdot s_R \rangle$  calculated with Lanczos ED for  $N = 40$  (thick lines:  $J_1 = -1$ , thin lines  $J_1 = +1$ ).

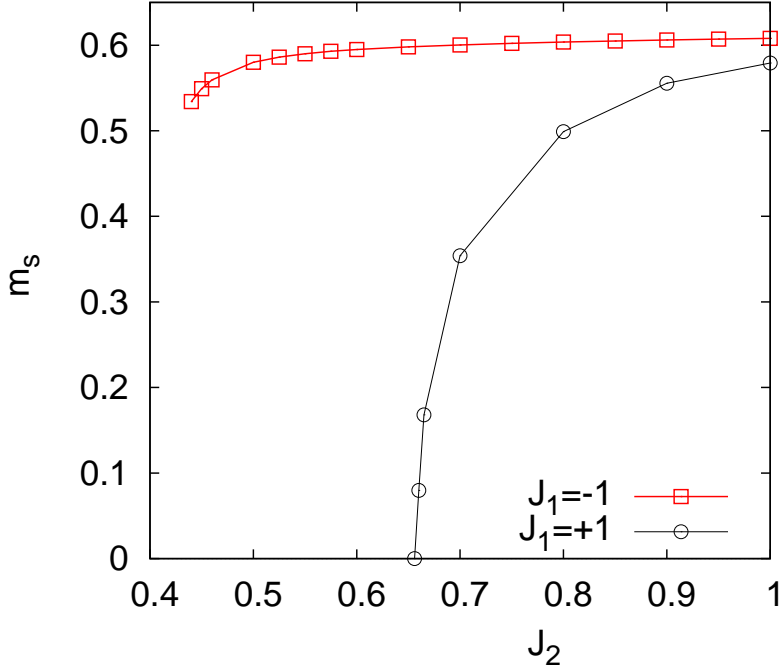


Figure 4: Extrapolated order parameters  $m_s$ , see Eq. (4), for the FM model ( $J_1 = -1$ ) and the AFM model ( $J_1 = +1$ ).

Following the lines of Refs. [4, 19] we use now the data for  $N = 20, 32, 36, 40$  to perform a finite-size extrapolation. Note that we do not include the data for the lattice with  $N = 16$  sites, since this lattice exhibits an anomalous behavior [4]. The finite-size extrapolation rules for the considered two-dimensional model are well known [45, 46]. The finite-size behavior of the GS energy is given by

$$\frac{E_0(N)}{N} = e_0 - \frac{\text{const.}}{N^{3/2}} + \dots \quad (3)$$

The extrapolated energy  $e_0$  is shown in Fig. 1. We use the intersection point between the extrapolated singlet GS energy  $e_0$  and the energy of the fully polarized FM GS to determine the transition point between both GS phases to  $J_2^{c1} = 0.393$ .

The order parameter for the collinear stripe LRO in the thermodynamic limit is defined as [4, 19]  $m_s = \sqrt{8} \lim_{N \rightarrow \infty} M_N(0, \pi)$ . The finite-size behavior of  $M_N(0, \pi)$  is given by

$$M_N^2(\pi, 0) = \frac{1}{8} m_s^2 + \frac{\text{const.}}{\sqrt{N}} + \dots \quad (4)$$

However, it is evident from Fig. 2 that the finite-size behavior of  $M_N^2(\pi, 0)$  becomes irregular at  $J_2 = 0.44$ , since we have  $M_{40}^2(\pi, 0) > M_{36}^2(\pi, 0)$  for  $J_2^{c1} < J_2 < 0.44$ . Hence, the extrapolation of  $M_N^2(\pi, 0)$  becomes inconclusive in that region. The results for  $m_s$  for  $J_2 \geq 0.44$  are shown in Fig. 4. For comparison we show also the extrapolated order parameter for the AFM model [19]. Although  $m_s$  becomes zero at  $J_2^{c2} \approx 0.66J_1$  for the AFM model, we do not find an indication for a magnetically disordered phase in the region above  $J_2 = 0.44$  for the FM model. However, we cannot exclude such a GS phase in the very small parameter region located between  $J_2 = 0.393$  and  $J_2 = 0.44$  from our ED data.

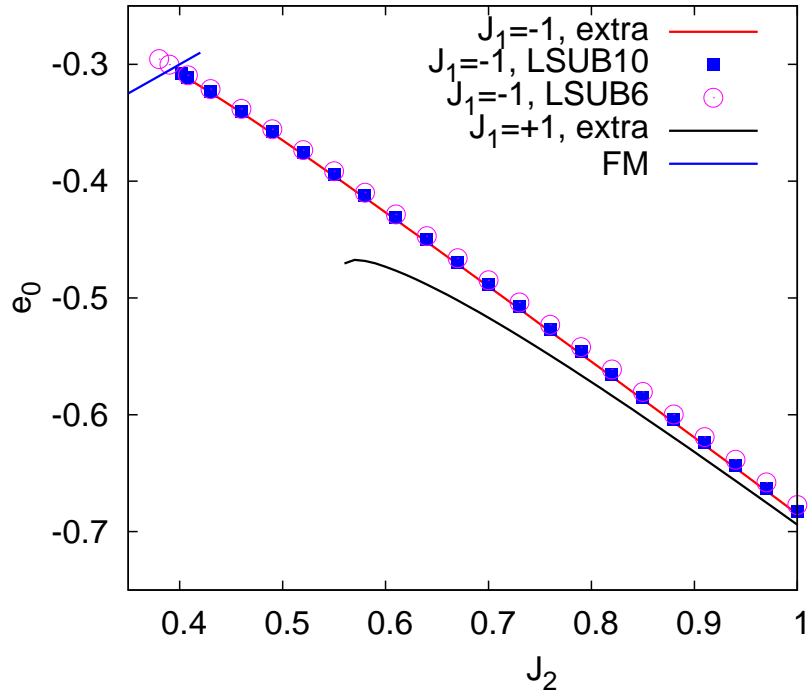


Figure 5: The GS energy per spin as function of  $J_2$  obtained by CCM-LSUB $n$  with  $n = 4, 6, 8, 10$  and extrapolated values in the limit  $n \rightarrow \infty$  using the extrapolation scheme  $e(n) = a_0 + a_1(1/n)^2 + a_2(1/n)^4$ . For the sake of comparison we show also the extrapolated GS energy for the AFM model [16]. The blue line shows the energy of the FM eigenstate.

### 3 Results of the coupled-cluster method (CCM) for the infinite square lattice

For the sake of brevity, we will illustrate only some important aspects of the CCM. The interested reader can find more details concerning the application of the CCM on the AFM  $J_1$ - $J_2$  in Refs. [8, 14–16]. For more general information on the methodology of the CCM, see, e.g., Refs. [47–49].

First we notice that the CCM approach automatically yields results in the thermodynamic limit  $N \rightarrow \infty$ . The starting point for a CCM calculation is the choice of a normalized reference (or model) state  $|\Phi\rangle$ . We then define a set of mutually commuting multispin creation operators  $C_I^+$  with respect to this state, which are themselves defined over a complete set of many-body configurations  $I$ . For the system under consideration here we choose one of the two degenerate classical collinear stripe states as the reference state. Next, we perform a rotation of the local axis of the spins such that all spins in the reference state align along the negative  $z$  axis. In the rotated coordinate frame the reference state reads  $|\Phi\rangle = |\downarrow|\downarrow|\downarrow|\dots$ , and we can treat each site equivalently. The corresponding multispin creation operators then can be written as  $C_I^+ = s_i^+, s_i^+ s_j^+, s_i^+ s_j^+ s_k^+, \dots$ , where the indices  $i, j, k, \dots$  denote arbitrary lattice sites.

The CCM parametrizations of the ket- and bra- GS's are given by

$$\begin{aligned} H|\Psi\rangle &= E|\Psi\rangle; & \langle\tilde{\Psi}|H &= E\langle\tilde{\Psi}|; \\ |\Psi\rangle &= e^S|\Phi\rangle, & S &= \sum_{I\neq 0} \mathcal{S}_I C_I^+; \\ \langle\tilde{\Psi}| &= \langle\Phi|\tilde{S}e^{-S}, & \tilde{S} &= 1 + \sum_{I\neq 0} \tilde{\mathcal{S}}_I C_I^-. \end{aligned} \quad (5)$$

We wish to determine the correlation coefficients  $\mathcal{S}_I$  and  $\tilde{\mathcal{S}}_I$  for the correlation operators  $S$  and  $\tilde{S}$ . By using the Schrödinger equation,  $H|\Psi\rangle = E|\Psi\rangle$ , we can write the GS energy as  $E = \langle\Phi|e^{-S}He^S|\Phi\rangle$ . The magnetic order parameter is given by

$$m_s = -\frac{1}{N_s} \sum_{i=1}^N \langle\tilde{\Psi}|s_i^z|\Psi\rangle, \quad (6)$$

where  $s_i^z$  is expressed in the rotated coordinate system and  $s = 1/2$  is the spin quantum number. To find the ket-state and bra-state correlation coefficients we have to solve the so-called CCM ket- and bra-state equations given by

$$\langle\Phi|C_I^- e^{-S} H e^S |\Phi\rangle = 0, \quad \forall I \neq 0, \quad (7)$$

$$\langle\Phi|\tilde{S} e^{-S} [H, C_I^+] e^S |\Phi\rangle = 0, \quad \forall I \neq 0. \quad (8)$$

Each ket- or bra-state equation belongs to a certain creation operator  $C_I^+ = s_i^+, s_i^+ s_j^+, s_i^+ s_j^+ s_k^+, \dots$ , i.e. it corresponds to a certain set (configuration) of lattice sites  $i, j, k, \dots$ .

For the considered quantum many-body model we have to use approximations in order to truncate the expansion of  $S$  and  $\tilde{S}$ . We use the well established LSUB $n$  scheme [14–16, 47–51] in which all multispin correlations in the correlation operators  $S$  and  $\tilde{S}$  over all distinct locales on the lattice defined by  $n$  or fewer contiguous sites are taken into account. For instance, within the LSUB4 approximation, multispin creation operators of one, two, three or four spins distributed on arbitrary clusters of four contiguous lattice sites are included. The number of these fundamental configurations can be reduced by using lattice symmetry and conservation laws. In the highest order of approximation considered here, namely the LSUB10 approximation, we have finally 45825

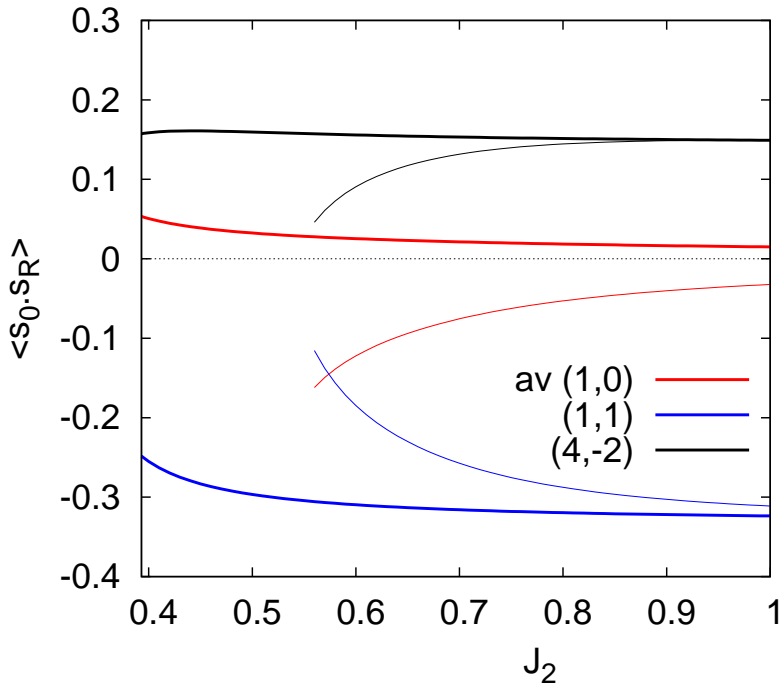


Figure 6: Selected spin-spin correlation functions  $\langle \mathbf{s}_0 \cdot \mathbf{s}_R \rangle$  calculated with CCM within LSUB6 approximation (thick lines:  $J_1 = -1$ , thin lines  $J_1 = +1$ ).

fundamental configurations for the collinear stripe reference state, yielding 45825 coupled nonlinear equations which have to be solved numerically.

The LSUB $n$  approximation becomes exact for  $n \rightarrow \infty$ , and so we can improve our results by extrapolating the “raw” LSUB $n$  data to  $n \rightarrow \infty$ . There is ample experience regarding how one should extrapolate the GS energy  $e_0(n)$  and the magnetic order parameter  $m_s(n)$ . For the GS energy per spin  $e_0(n) = a_0 + a_1(1/n)^2 + a_2(1/n)^4$  is a reasonable well-tested extrapolation ansatz [13–16, 48–51]. An appropriate extrapolation rule for the magnetic order parameter is  $m_s(n) = b_0 + b_1(1/n)^{1/2} + b_2(1/n)^{3/2}$  [14–16]. Moreover, we know from Refs. [14–16] that the lowest level of approximation called the LSUB2 approximation conforms poorly to these rules. Hence, as in previous calculations [14–16], we exclude LSUB2 data from the extrapolations.

Note that starting from large  $J_2$  the solution of the CCM-LSUB10 equations can be traced until  $J_2 = 0.402$ , only. For  $J_2 < 0.402$  no CCM-LSUB10 solutions with respect to the collinear stripe reference state could be found. This could be related to the complexity of the set of 45825 coupled equations and the fact that the fully polarized FM state is a low-lying excitation very close to the true GS for  $J_2 \sim 0.4$ . However, we cannot exclude the possibility that this problem might also be an indication that the collinear stripe order is not a good description for the true GS for  $J_2$  values very close to the transition to the FM GS.

In Fig. 5 we show the GS energy per site for the LSUB6 and LSUB10 approximations, as well as the extrapolated GS energy ( $n \rightarrow \infty$ ). The numerical CCM-LSUB $n$  data demonstrate, that the difference between the various LSUB $n$  data is very small (see Fig. 5). As a result, the extrapolated GS energy almost coincides with LSUB10 data (in fact, the difference is less than 0.4%). Moreover, the difference between the extrapolated CCM energy and the finite-size extrapolated ED energy is less than 1% in the whole parameter region. Hence, we conclude that the GS energy data presented in this paper for the FM  $J_1$ - $J_2$  model are very accurate. We again use the intersection

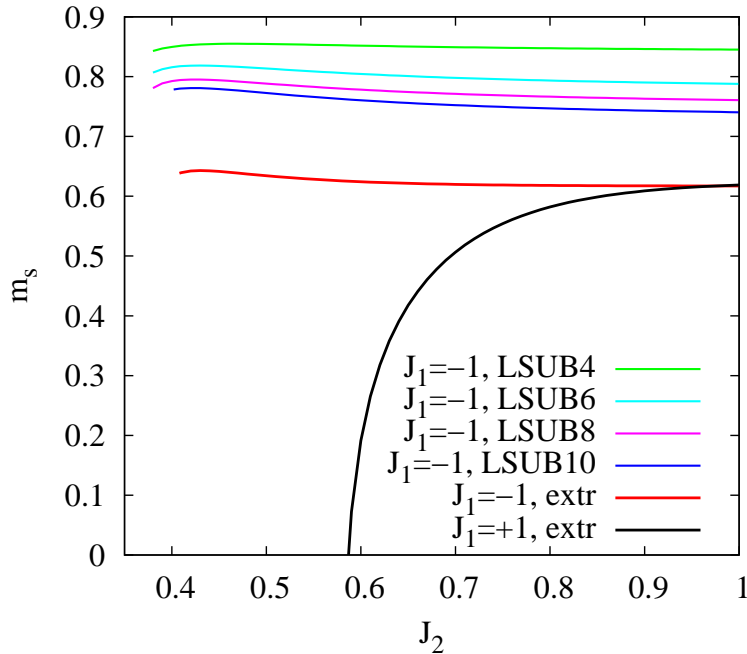


Figure 7: Magnetic order parameter  $m_s$  versus  $J_2$  obtained by CCM-LSUB $n$  with  $n = 4, 6, 8, 10$  and its extrapolated values ( $n \rightarrow \infty$ ) using the extrapolation scheme  $m_s(n) = b_0 + b_1(1/n)^{1/2} + b_2(1/n)^{3/2}$ . By way of comparison we show also the extrapolated collinear stripe order parameter ( $n \rightarrow \infty$ ) for the AFM model ( $J_1 = +1$ ).

point of the energies in order to find an estimate for the transition point  $J_2^{c1}$  to the FM GS. We find that  $J_2^{c1} = 0.395$  for the LSUB6 approximation and this is shown in Fig. 5. We find also that  $J_2^{c1} = 0.394$  and  $J_2^{c1} = 0.398$  for the LSUB8 and LSUB4 approximations, respectively (not shown in Fig. 5). As the difference between the LUSB6 and LSUB8 results for  $J_2^{c1}$  is already very small we may choose the LUSB8 value,  $J_2^{c1} = 0.394$ , as the CCM estimate for the transition point. This CCM critical value is in excellent agreement with the ED estimate  $J_2^{c1} = 0.393$  (see above). We also compare the GS energies for the FM and the AFM models in Fig. 5. As for the ED method, the deviation in energies between the two models (i.e., negative and positive  $J_1$ ) becomes substantial at around  $J_2 = 0.6$ .

We also present the CCM results for spin-spin correlation functions for the FM as well as the AFM model in Fig. 6, where we have shown the same correlation functions as in Fig. 3. Recall that one of the two degenerate collinear stripe states has to be chosen as CCM reference state. As a result the NN correlation functions  $\langle \mathbf{s}_0 \cdot \mathbf{s}_{\mathbf{R}} \rangle$ ,  $\mathbf{R} = (1, 0)$ , and  $\langle \mathbf{s}_0 \cdot \mathbf{s}_{\mathbf{R}} \rangle$ ,  $\mathbf{R} = (0, 1)$ , are different, whereas, e.g., all NNN correlation functions are the same. Hence, we show in Fig. 6 the averaged NN correlation function. For the FM model the agreement of the CCM correlation functions with the ED data is excellent, see Figs. 3 and 6. For the AFM model there is a noticeable difference for  $J_2 < 0.59$ . In particular, the steep decrease in the correlation functions at  $J_2 = 0.59$  present in the ED data for the AFM model, cf. Ref. [19], is not observed in the CCM LSUB6 data. For  $J_2 < 0.59$  most likely no magnetic LRO exists for the AFM model [16]. Therefore it is not surprising that the CCM solution in a finite order of LSUB $n$  approximation based on the collinear stripe reference state does not provide quantitatively precise results for the correlation functions inside the magnetically disordered phase.

Last but not least, we present results for the collinear stripe order parameter  $m_s$  calculated

by the CCM via Eq. (6) in Fig. 7. For the order parameter, the CCM-LSUB $n$  results depend on the approximation level  $n$  more strongly than for the GS energy. Hence, it is more important to extrapolate them in the limit  $n \rightarrow \infty$ . By comparing the correlation functions and the order parameter of the FM model with the AFM model, it is again obvious that both models behave similarly for larger  $J_2$ . However, there are significant differences for  $J_2 \lesssim 0.6$  between both models. Although the CCM result for the AFM model clearly shows the breakdown of the semiclassical collinear magnetic LRO around  $J_2 = 0.6$  (the CCM estimate for the critical frustration is  $J_2^{c2} \approx 0.59$  [16]), the spin-spin correlation functions and the order parameter for the FM model stay almost constant over the whole parameter region shown in Fig. 7. Again, we obtain good agreement of the order parameter between the ED data and the CCM data in a wide parameter range, cf. Figs. 4 and 7. Finally, we come to a similar conclusion as in Sec. 2 that we do not find an indication for the breakdown of the collinear stripe magnetic LRO until  $J_2 \sim 0.4$  for the FM model.

## 4 Summary

In this paper we have presented results on the GS magnetic ordering of the  $J_1$ - $J_2$  spin-1/2 Heisenberg magnet with FM NN exchange  $J_1 = -1$  on the square lattice obtained by Lanczos ED as well as the CCM. In agreement with previous studies [29–31, 34, 37, 38] we obtain values for the transition point  $J_2^{c1}$  at which the fully polarized FM GS (present for small  $J_2$ ) breaks down,  $J_2^{c1} = 0.393|J_1|$  (ED) and  $J_2^{c1} = 0.394|J_1|$  (CCM).

In contrast to previous studies [29–31, 34] we do not find indications for the breakdown of the semiclassical collinear magnetic LRO (present for large  $J_2$ ) at about  $J_2 = 0.6|J_1|$ , rather this magnetic LRO seems to be stable till  $J_2 \sim 0.4|J_1|$ .

Although our results are in favour of semiclassical magnetic GS long-range order for a wide range of frustrating exchange  $J_2$ , the low-lying excitations and, as a consequence, the low-temperature thermodynamics might be strongly influenced by frustration. This becomes increasingly important when approaching the transition to the FM GS at  $J_2^{c1} \approx 0.4|J_1|$ , see e.g. Ref. [37]. For  $J_2 \gtrsim J_2^{c1}$  the FM multiplet becomes a low-lying excitation, and so an additional low-energy scale will appear leading, e.g., to an extra low-temperature peak in the specific heat, see, e.g., Refs. [29, 52, 53].

Stimulated by the recent experimental activities and the related search for new square-lattice materials near the quantum critical point of the  $J_1$ - $J_2$  model, the issue of low-lying excitations and their relevance for the thermodynamic properties should be investigated in future studies in more detail.

**Acknowledgement:** We thank S.E. Krüger and R. Zinke for valuable discussions. This work was supported by the DFG (Ri615/16-1).

## References

- [1] P. Chandra and B. Douçot, Phys. Rev. B **38**, 9335 (1988).
- [2] E. Dagotto and A. Moreo, Phys. Rev. Lett. **63**, 2148 (1989).
- [3] F. Figueirido, A. Karlhede, S. Kivelson, S. Sondhi, M. Rocek, and D.S. Rokhsar, Phys. Rev. B **41**, 4619 (1990).
- [4] H.J. Schulz and T.A.L. Ziman, Europhys. Lett. **18**, 355 (1992); H.J. Schulz, T.A.L. Ziman, and D. Poilblanc, J. Phys. I **6**, 675 (1996).

- [5] J. Richter, Phys. Rev. B **47**, 5794 (1993).
- [6] J. Richter, N.B. Ivanov, and K. Retzlaff, Europhys. Lett. **25**, 545 (1994).
- [7] A. E. Trumper, L. O. Manuel, C. J. Gazza, and H. A. Ceccatto, Phys. Rev. Lett. **78**, 2216 (1997).
- [8] R.F. Bishop, D.J.J. Farnell, and J.B. Parkinson, Phys. Rev. B **58**, 6394 (1998).
- [9] L. Capriotti, F. Becca, A. Parola, and S. Sorella, Phys. Rev. Lett. **87**, 097201 (2001).
- [10] L. Siurakshina, D. Ihle, and R. Hayn, Phys. Rev. B **64**, 104406 (2001).
- [11] R.R.P. Singh, Weihong Zheng, J. Oitmaa, O.P. Sushkov, and C.J. Hamer, Phys. Rev. Lett. **91**, 017201 (2003).
- [12] J. Sirker, Z. Weihong, O. P. Sushkov, and J. Oitmaa, Phys. Rev. B **73**, 184420 (2006).
- [13] D. Schmalfuß, R. Darradi, J. Richter, J. Schulenburg, and D. Ihle, Phys. Rev. Lett. **97**, 157201 (2006).
- [14] R.F. Bishop, P.H.Y. Li, R. Darradi, and J. Richter, J. Phys.: Condens. Matter **20**, 255251 (2008).
- [15] R.F. Bishop, P.H.Y. Li, R. Darradi, J. Schulenburg and J. Richter, Phys. Rev. B **78**, 054412 (2008).
- [16] R. Darradi, O. Derzhko, R. Zinke, J. Schulenburg, S. E. Krüger, and J. Richter, Phys. Rev. B **78**, 214415 (2008).
- [17] T. Pardini and R.R.P. Singh, Phys. Rev. B **79**, 094413 (2009).
- [18] V. Murg, F. Verstraete, and J. I. Cirac, Phys. Rev. B **79**, 195119 (2009).
- [19] J. Richter and J. Schulenburg, Eur. Phys. J. B **73**, 117 (2010).
- [20] J. Reuther and P. Woelfle, arXiv:0912.0860.
- [21] E. E. Kaul, H. Rosner, N. Shannon, R.V. Shpanchenko, and C. Geibel, J. Magn. Magn. Mater. **272-276(II)**, 922 (2004).
- [22] M. Skoulatos, J.P. Goff, N. Shannon, E.E. Kaul, C. Geibel, A.P. Murani, M. Enderle, and A.R. Wildes, J. Magn. Magn. Mater. **310**, 1257 (2007).
- [23] P. Carretta, M. Filibian, R. Nath, C. Geibel, and P. J. C. King, Phys. Rev. B **79**, 224432 (2009).
- [24] M. Skoulatos, J.P. Goff, C. Geibel, E.E. Kaul, R. Nath, N. Shannon, B. Schmidt, A.P. Murani, P.P. Deen, M. Enderle, and A.R. Wildes, arXiv:0909.0702.
- [25] H. Kageyama, T. Kitano, N. Oba, M. Nishi, S. Nagai, K. Hirota, L. Viciu, J.B. Wiley, J. Yasuda, Y. Baba, Y. Ajiro, and K. Yoshimura, J. Phys. Soc. Jpn. **74**, 1702 (2005).
- [26] A.A. Tsirlin and H. Rosner, Phys. Rev. B **79** 214417 (2009).

- [27] A.A. Tsirlin, B. Schmidt, Y. Skourski, R. Nath, C. Geibel, and H. Rosner, *Phys. Rev. B* **80** 132407 (2009).
- [28] R. Nath, A.A. Tsirlin, H. Rosner, and C. Geibel, *Phys. Rev. B* **78** 064422 (2008).
- [29] N. Shannon, B. Schmidt, K. Penc, and P. Thalmeier, *Eur. Phys. J. B* **38**, 599 (2004).
- [30] N. Shannon, T. Momoi, and P. Sindzingre, *Phys. Rev. Lett.* **96**, 027213 (2006).
- [31] P. Sindzingre, N. Shannon and T. Momoi, *J. Magn. Magn. Mat.* **310**, 1340 (2007).
- [32] B. Schmidt, N. Shannon, and P. Thalmeier, *J. Phys. Cond. Mat.* **19**, 145211 (2007).
- [33] B. Schmidt, N. Shannon, and P. Thalmeier, *J. Magn. Magn. Mater.* **310**, 1231 (2007).
- [34] J.R. Viana and J.R. de Sousa, *Phys. Rev. B* **75**, 052403 (2007).
- [35] P. Sindzingre, L. Seabra, N. Shannon, and T. Momoi, *J. Phys.: Conf. Series* **145**, 012048 (2009).
- [36] P. Sindzingre, N. Shannon, and T. Momoi, arXiv:0907.4163.
- [37] M. Härtel, J. Richter, D. Ihle, and S.-L. Drechsler, arXiv:1001.1222.
- [38] D. V. Dmitriev, V. Ya. Krivnov, and A. A. Ovchinnikov, *Phys. Rev. B* **55**, 3620 (1997).
- [39] T. Munehisa and Y. Munehisa, *J. Phys: Condensed Matter* **19**, 196202 (2007).
- [40] T. Kashima and M.Imada, *J. Phys. Soc. Jpn.* **70**, 3052 (2001).
- [41] J. Richter, J. Schulenburg, and A. Honecker, in: *Quantum Magnetism*, ed by U. Schollwöck, J. Richter, D.J.J. Farnell, R.F. Bishop, *Lecture Notes in Physics* **645**, p. 85 (Springer, Berlin, 2004).
- [42] A. Läuchli, J.C. Domenge, C. Lhuillier, P. Sindzingre, and M. Troyer, *Phys. Rev. Lett.* **95**, 137206 (2005).
- [43] J. Richter, J. Schulenburg, A. Honecker, and D. Schmalfuß, *Phys. Rev. B* **70**, 174454 (2004).
- [44] J. Schulenburg, A. Honecker, J. Schnack, J. Richter, and H. - J. Schmidt, *Phys. Rev. Lett.* **88**, 167207 (2002); A. Honecker, J. Schulenburg, and J.Richter, *J. Phys.: Condens. Matter* **16**, S749 (2004).
- [45] H. Neuberger and T. Ziman, *Phys. Rev. B* **39**, 2608 (1989).
- [46] P. Hasenfratz and F. Niedermayer, *Z. Phys. B: Condens. Matter* **92**, 91 (1993).
- [47] C. Zeng, D. J. J. Farnell, and R. F. Bishop, *J. Stat. Phys.* **90**, 327 (1998).
- [48] R. F. Bishop, D. J. J. Farnell, S. E. Krüger, J. B. Parkinson, and J. Richter, *J. Phys.: Condens. Matter* **12**, 6877 (2000).
- [49] D. J. J. Farnell and R. F. Bishop, in *Quantum Magnetism*, *Lecture Notes in Physics Vol. 645*, edited by U. Schollwöck, J. Richter, D. J. J. Farnell, and R. F. Bishop (Springer, Berlin, 2004), p. 307.

- [50] S. E. Krüger, J. Richter, J. Schulenburg, D. J. J. Farnell, and R. F. Bishop, Phys. Rev. B **61**, 14607 (2000).
- [51] R. Darradi, J. Richter, and D.J.J. Farnell, Phys. Rev. B **72**, 104425 (2005).
- [52] F. Heidrich-Meisner, A. Honecker, and T. Vekua, Phys. Rev. B **74**, 020403(R) (2006).
- [53] H. T. Lu, Y. J. Wang, Shaojin Qin, and T. Xiang, Phys. Rev. B **74**, 134425 (2006).